Environmental Science and Pollution Research (2019) 26:10631–10640
https://doi.org/10.1007/s11356-019-04528-0

RESEARCH ARTICLE

A novel nano zero-valent iron biomaterial for chromium (Cr^{6+} to Cr^{3+}) reduction

Utsav Dalal[1] · Sivamohan N. Reddy[1]

Received: 3 November 2018 / Accepted: 6 February 2019 / Published online: 15 February 2019

Abstract

This research work aims to develop a biomaterial entrapped with iron nanoparticles by green synthesis method in which biomass act as both reducing and capping agent. Iron nanoparticles embedded in *Citrus limetta* peels were characterised using ICP-MS for determination of metal loading, XRD, XPS for crystallinity and oxidation states, TEM followed by FESEM-EDS for particle size and morphology. Sizes of nanoparticles were found to be in the range of 4–70 nm. Batch experiments were conducted to study the effect of different parameters such as contact time, amount of biomaterial and volume of chromium(VI) solution for 2500 mg L^{-1} of Cr(VI). Complete reduction was attained for a contact time of 5 min with 1.5 g of biomaterial for initial concentration of 2500 mg L^{-1}. The experimental results inferred that 1 g of biomaterial completely reduced 33 mg of hexavalent Cr to trivalent Cr. XRD and XPS revealed that iron nanoparticles are in amorphous form while XPS confirms Fe^0 state. The transition of Fe^0 to Fe^{2+}/Fe^{3+} during the treatment with chromium solution confirms the reduction of Cr^{6+} to Cr^{3+}.

Keywords *Citrus limetta* · Biosynthesis · Iron nanoparticles · Biomaterial · Chromium reduction

Introduction

The contamination of water with various toxic chemicals and their treatment has become a major environment problem. The use of pesticides and industrialisation lead to pollution due to the consumption of variety of chemicals (Madhavi et al. 2013). Heavy metals are identified as major environmental pollutants which include arsenic, chromium, mercury and lead. These are toxic in nature and found to be harmful for both humans as well as environment (Ray and Kanti Ray 2009). Industrial wastewater from electroplating, tanning industries, steel plants and manufacturing of electronic products contain high amount of heavy metals (Yin et al. 2017). These industrial effluents entering into the water streams are the main source of heavy metal water pollution. Chromium exists in two stable oxidation states Cr^{3+} and Cr^{6+}, of which hexavalent chromium is known for its toxicity as it is carcinogenic, mutagenic and teratogenic in nature (Costa and Klein 2006; Miretzky and Cirelli 2010; Yuan et al. 2010).

Various methods are in practice for the removal of Cr(VI) from industrial wastewater such as electrochemical ion exchange (Dharnaik and Ghosh 2014), membrane separation (Gaikwad and Balomajumder 2018), chemical reduction (Johnson et al. 2017; Zhou et al. 2018) and adsorption (Kumari et al. 2015). These conventional methods are labour-intensive, expensive, energy-consuming and hazardous to the environment (Narayanan and Sakthivel 2010; Gan and Li 2012). Cr(VI) is normally found as oxyanions (CrO_4^{2-} and $Cr_2O_7^{2-}$) which makes precipitation of chromium difficult using conventional methods. Other challenges which these methods face are low reduction and incompetent removal of metals from solution. Furthermore electrochemical ion-exchange and membrane separation techniques use membranes/high-pressure equipment and electricity which makes treatment expensive and labour-intensive (Dharnaik and Ghosh 2014). Adsorption technique has emerged as a promising technology due to its ease of operation, availability, low cost and capability of producing high-quality water (Chen et al. 2016). Activated carbon in powder or granular form has been successfully proved for the removal of heavy metals from wastewater (Nayak et al. 2017; Kim et al. 2018). However, chemicals ($ZnCl_2$, KOH) used for the activation process pose secondary environmental pollution

Responsible editor: Tito Roberto Cadaval Jr

✉ Sivamohan N. Reddy
nsiva.fch@iitr.ac.in

[1] Department of Chemical Engineering, Indian Institute of Technology Roorkee, Roorkee, Uttarakhand 247 667, India

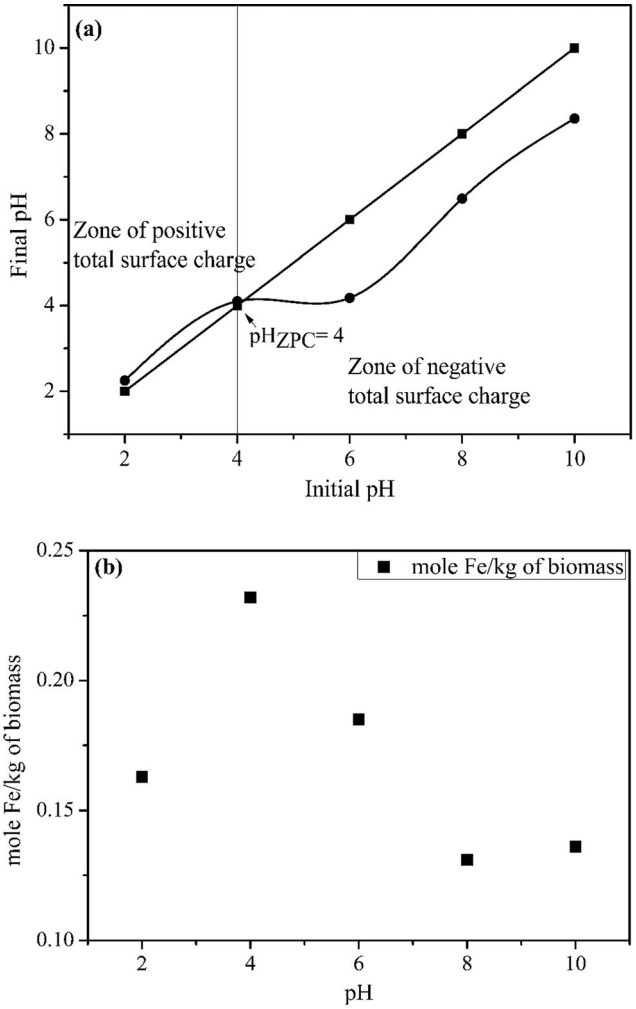

Fig. 1 **a** Determination of zero-point charge where maximum metal loading occurs, **b** metal loading on to the biomass with respect to pH value

problem and overall make it a costly process (Chen et al. 2016). An alternate approach is to use biomass for the adsorption which is readily available, low cost and which is often considered as waste. It is well known that cellulosic agricultural has the capability for adsorption of heavy metals. Adsorption capacity of biomass was less than activated carbon. However, when zero-valent iron was added to biomass, toxic metals can be reduced effectively (Garg et al. 2009). Variety of biomasses has been investigated for their use in wastewater treatment for the removal of heavy metals which are cheap and readily available (Vivek Narayanan and Ganesan 2009). The application of biomass with significant specificity for the adsorption of Cr(VI) gained the attention in recent years. Researchers have found that sugarcane bagasse, corncobs, eucalyptus bark and Jatropha oil cake as sustainable adsorbents for chromium, lead, arsenic and mercury removal (Garg et al. 2009).

In recent years, iron nanoparticles have been successfully used to treat wastewater containing heavy metals. Iron nanoparticles have high reactive surface area, which results in completion of reactions (Li et al. 2006). Researchers have been developing porous materials which enhance the dispersibility of iron nanoparticles. Bentonite (Bhattacharyya and Gupta 2008), zeolite (Li et al. 2007) and chitosan (Geng et al. 2009) have been used for wastewater remediation. Bentonite is a low-cost efficient adsorbent, chemically and mechanically stable which possesses high potential for heavy metal removal from wastewaters. In the recent years, researchers have developed an alternative method, which uses plants extract as reducing agent for synthesis of iron nanoparticles as an alternate to expensive conventional reducing agents (Fahmy et al. 2018). The most recent technologies for synthesis of iron nanoparticle make use of vegetables, fruits and organic waste extracts. These extracts are mixed with iron salt solution without any further requirement of chemicals/energy. Green iron nanoparticles are formed with a special reaction between iron and polyphenols found in plant extract, which are defined as the colour change from pale green to dark green or black colour (Hoag et al. 2009). Plant extract like tea extract (Machado et al. 2013), sorghum bran (Njagi et al. 2011), *Eucalyptus globulus* leaf extract (Madhavi et al. 2013), banana peel extract (Thakur and Karak 2014), urtica dioca leaf extract (Ebrahiminezhad et al. 2017) and orange peel (López-Téllez et al. 2011) have been successfully used for synthesis of iron nanoparticles.

In the current work, raw *Citrus limetta* peels have been used for the synthesis of iron nanoparticles. Peels are considered as bio-waste which are cheap, readily available and biodegradable. Peels act as good reducing agent as well as capping agent for the reduction of iron ions to nanoparticles. Iron nanoparticles being highly reactive tend to agglomerate increasing its particle size and making it unsuitable for the reactions as surface to volume ratio increases (Geng et al. 2009). The developed biomaterial acts as supporting medium as well as reducing agent for metals. Secondly, the material can be easily regenerated with sustained performance. Optimum pH was determined for maximum loading of iron onto the peels and later the iron embedded biomaterial was tested for the remediation of hexavalent chromium. The impact of key parameters such as contact time, amount of biomaterial and initial chromium concentration on the removal of hexavalent chromium has been studied. The developed material reduces more toxic Cr^{6+} to less toxic Cr^{3+} that would be desorbed from the material sequentially. This enables to quickly regenerate the developed material without any addition/generation toxic components.

Material and methods

Biomass and chemicals

Citrus limetta peels were collected from nearby juice centre located in Roorkee, India. Initially, these peels were washed with double distilled water to remove any

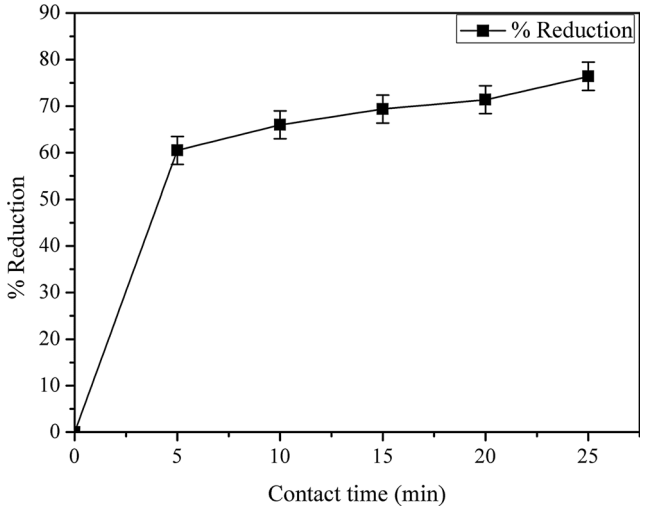

Fig. 2 Reduction % of Cr(VI) vs contact time

impurities. Washed peels were incised into small pieces and further rewashed with double distilled water. These small-pieced peels were milled and sieved into fine powder. Metal precursor (ferrous sulphate, $FeSO_4.7H_2O$), nitric acid and sodium hydroxide were purchased form Sigma-Aldrich, India.

Impregnation of iron onto biomass and determination of pHzpc

The pH of metal aqueous solution exerts a great influence on the formation of nanoparticles. The fluctuation in pH alters the charge of phytochemicals which are present in the biomass. This in turn may affect their ability to reduce and bind metal ions (Sathishkumar et al. 2010). To study the maximum loading of metal onto the biomass, pH was varied. This method infers that about zero-point charge of the solution maximum loading of metal will be attained (Richardson et al. 2010).

To know the effect of pH on metal loading, 0.1 M solution of $FeSO_4.7H_2O$ was used for impregnation at different pH of 2, 4, 6, 8 and 10 by adjusting it with suitable acid and base. The impregnation of metal loading was conducted for a period of 48 h. As pH fluctuates during impregnation, it was monitored and the deviation was nullified to attain the initial pH using acid/base. After impregnation, biomass was filtered using filter paper. Filtered biomass was gently washed with milli-pore water thrice and then dried at 105 °C in an oven. The metal loading in the impregnated biomass was determined by inductively coupled plasma mass spectroscopy (ICP-MS). At pHzpc, 20 g of fruit peels (powder form) was impregnated with 200 mL of 0.1 M iron salt solution for 48 h. Solid biomass after filtration was dried and biomaterial was named as CL-FeNPs and filtrate (liquid extract) was stored for further use.

Characterisation

Metal loading onto the biomass was determined by ICP-MS (Perkin Elmer, Model- ELAN DRC-e). Before analysis, samples were digested with the mixture of hydrochloric acid and hydrogen peroxide in 3:2 ratio and was further diluted to the concentration of ppb. XRD (D8-Adavnace) was performed on X-ray diffractometer, operated at 40KV and 30 mA. The pattern was recorded by Cu-Kα radiation with $\lambda = 0.15406$ nm. XRD spectra were analysed using X'PERT Highscore software. Surface area was determined by the multipoint Brunauer-Emmett-Teller (BET) method using a Micromeritics Accelerated Surface Area and Porosimetry (ASAP 2020, USA) instrument. Prior to analysis, the material was degassed under vacuum for 4 h to make it moisture free. To determine the oxidation states of the metals, XPS (PHI 5000 VersaProbe III) was performed. Elemental composition and surface morphology along with the distribution of elements at the imaged area and particle size distribution were examined using SEM-EDX (FE-SEM QUANTA 200 FEG) and high-resolution transmission electron microscopy (HRTEM, Model no: JEOL-JEM-3200FS). For TEM analysis, powdered sample was ultrasonicated for 30 min in ethanol so that iron particles get isolated and a small drop of sample was dropped on 200 mesh carbon-coated copper grid which was further dried before analysis.

Chromium batch experiments

Batch studies were performed to examine the extent of reduction of chromium(VI) in a series of trials with different parameters (namely contact time, quantity of biomaterial, initial

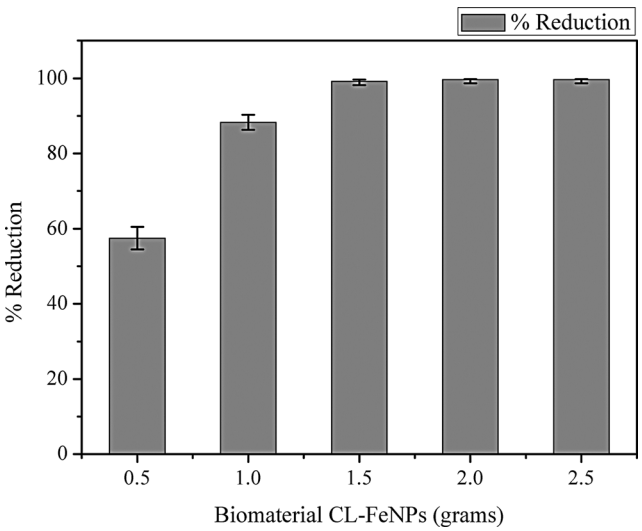

Fig. 3 Reduction % of Cr(VI) vs loading of biomaterial

Table 1 Reduction % of chromium(VI) with increase in initial chromium concentration and quantity of chromium solution of concentration 2500 mg L^{-1}

Weight of biomaterial, 1 g			Weight of biomaterial, 1.5 g	
Sno	Initial chromium concentration (mg L^{-1})	% reduction	Volume of chromium solution of 2500 mg L^{-1}	% reduction
1	500	98.9 ± 0.3	20	79.8 ± 0.6
2	1000	99.2 ± 0.2	40	44.9 ± 0.9
3	1500	99.4 ± 0.3	60	35.8 ± 0.7
4	2000	95.3 ± 0.7	80	21.4 ± 1
5	2500	87.4 ± 0.5	100	20.7 ± 1.5

chromium concentration and volume of stock solution). An initial hexavalent chromium concentration of 2500 mg L^{-1} was prepared as stock solution and was used throughout the experiments. Initially, effect of contact time was studied with time interval of 5, 10, 15, 20 and 25 min. Parameters like biomaterial dosage (0.5, 1, 1.5, 2 and 2.5 g), volume of chromium solution (20, 40, 60, 80 and 100 mL), initial chromium(VI) concentration (500, 1000, 1500, 2000 and 2500 mg L^{-1}) and volume of liquid extract were tested. Finally, a comparative study was done between freshly prepared and regenerated biomaterial. These comparative experiments were performed using 2.5 g of biomaterial with 100 mL of 1000 mg L^{-1} chromium solution. All the experiments were done at room temperature and atmospheric pressure. Experiments were conducted twice and the average values of the removal efficiencies were reported here. The deviation in the reduction values was found to be close to 4%. The amount of Cr(VI) reduced per unit gram of the biomaterial was calculated using expression,

$$q = \frac{(C_o - C_t)V}{m} \quad (1)$$

where C_0 and C_t are initial and final *C*r(VI) concentration and '*m*' is the amount of biomaterial in grams in *V* litres of Cr(VI) solution. The percentage reduction '*R*' was calculated using the expression

$$R = \left[\frac{C_o - C_t}{C_o}\right] 100 \quad (2)$$

Chromium detection using colorimetric method

A well-known colorimetric method was used to analyse the chromium(VI) concentration of the samples. The chemical 1,5-diphenyl carbazide forms a complex when reacted with Cr(VI) in acidic medium, which appears as pink colour in the solution. After the reaction, it was measured at 540 nm using UV-spectrophotometer (Model UV-1800 Shimadzu company).

Results and discussion

Zero-point charge and ICP-MS analysis

The pH of the solution was varied to determine the optimum pH at which the maximum metal loading occurs. The point of zero charge can be known by plotting a graph between initial and final pH. The point where this curve crosses the 45° line is usually termed as zero-point charge. Figure 1a infers that optimum pH for metal loading on *Citrus limetta* occurs at pH 4. If the $pH < pH_{ZPC}$, then the solution becomes positively charged, the condition in which H^+ and free metal cations compete for sorbent active sites which reduces the metal loading (Richardson et al. 2010). When the $pH > pH_{ZPC}$, then the solution becomes negatively charged which forms hydroxides of metal salt resulting in the increase of the metal loading onto the biomass. Metal content was quantitatively determined using ICP-MS. Figure 1b also confirms that maximum loading of metal occurs at pH 4 with about 0.232 mol of Fe/kg of biomass which is an agreement with the pH variation analysis. A little increase in

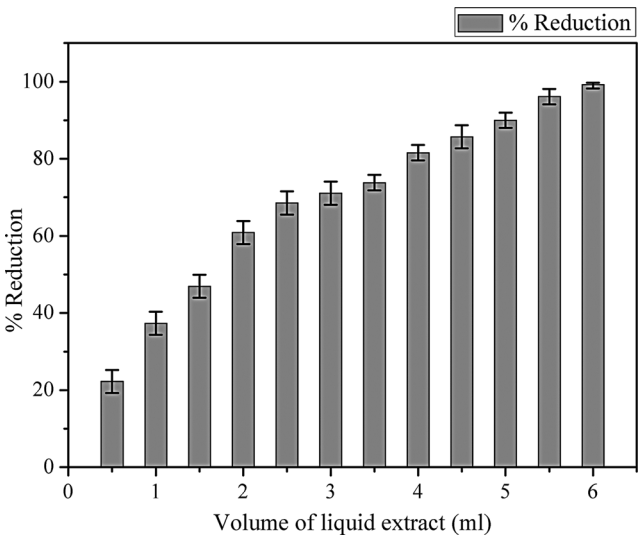

Fig. 4 Influence of varying volume of liquid extract on reduction % of Cr(VI)

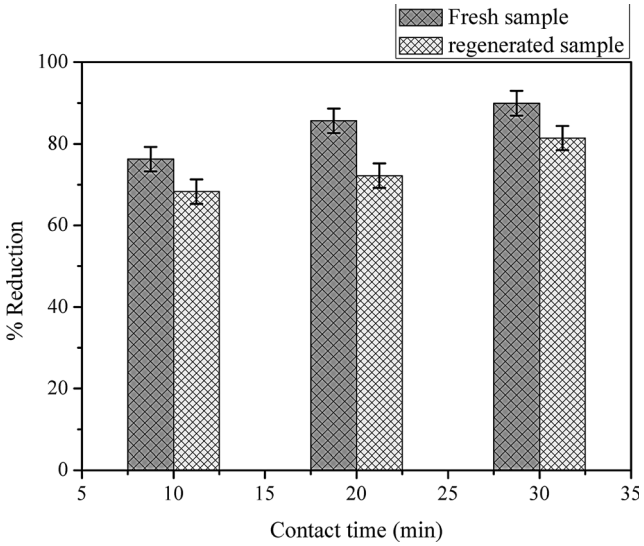

Fig. 5 Comparative study between fresh biomaterial sample and regenerated sample vs residence time

metal loading was observed at pH 10, which is due to the precipitation of $Fe(OH)_2$ and its deposition on the biomaterial.

Effect of contact time

To study the effect of contact time on Cr(VI) reduction, 1 g of biomaterial was added to 20 mL of chromium stock solution. Sample was collected at regular intervals of 5, 10, 15, 20 and 25 min. From Fig. 2, it was clear that with the increase in contact time, percentage reduction of Cr(VI) increases but only up to a certain point. Initially 63% reduction was observed for 5 min of contact time. But as reaction proceeds, metallic iron oxidises to iron(III) oxide in the form of precipitate ultimately

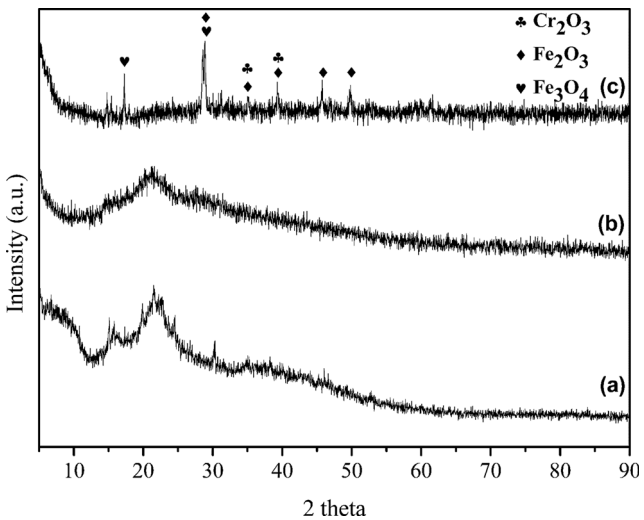

Fig. 6 XRD spectrum of (a) fresh *Citrus limetta* peels, (b) biomaterial CL-FeNPs and (c) biomaterial CL-FeNPS treated with chromium solution

blocking the active sites. The reduction percentage of 66, 69, 71 and 73% was recorded for 10, 15, 20 and 25 min of contact time respectively. It can be inferred that at initial stages, reduction rate was high and later it attains asymptotic value at higher contact time (Karthikeyan et al. 2005). Therefore, the contact time of 5 min was taken as optimum contact time for the reduction of Cr(VI).

Effect of amount of biomaterial

To study the effect of biomaterial dosage on reduction of Cr(VI), the quantity of biomaterial was varied from 0.5 to 2.5 g. Figure 3 infers biomaterial loading enhances the reduction percentage. With the increase in amount of biomaterial, the reaction sites for the reaction of Cr(VI) ions increase which ultimately contribute to higher reduction. Complete (100% of Cr(VI)) reduction was achieved with 1.5 g of biomaterial for a concentration of 2500 mg L^{-1} of chromium solution. From the experiments, it has been found that a maximum reduction capacity of 33.3 mg of chromium(VI)/g of biomaterial was attained within 5 min at pH 7.

Effect of initial concentration of chromium and volume of chromium stock solution

To study the effect of initial chromium concentration on reduction of Cr(VI), the concentration of chromium was varied from 500 to 2500 mg L^{-1}. Then a fixed quantity of biomass i.e. 1 g of biomaterial was stirred for a contact time of 5 min. Due to more active reactive sites in the synthesised biomaterial, complete (100%) reduction was observed up to 1500 mg L^{-1}, 95% was recorded for 2000 mg L^{-1} and 87% for 2500 mg L^{-1} as shown in Table 1. The volume of chromium stock solution (20, 40, 60, 80 and 100 mL) was also changed to study the chromium reduction for 5 min and 1.5 g. Table 1 shows that with the increase in the volume of stock solution, percentage reduction of Cr(VI) decreases. Complete reduction was observed for only 20 mL of solution. But with the increase in volume of the chromium solution, reduction % decreases to 45, 35, 21 and 20 for 40, 60, 80 and 100 mL respectively. Initial ratio of available surface to initial chromium concentration is high and as the concentration increases, this ratio decreases resulting in lower Cr(VI) reduction. Table 1 confirms that for a given quantity of biomaterial, chromium ion concentration is inversely proportional to reduction percentage.

Effect of volume of iron-dispersed liquid extract

It was observed from Fig. 4 that the increase in volume of liquid extract increases reduction of chromium(VI). DLS analysis of iron-dispersed liquid extract was done and the mean

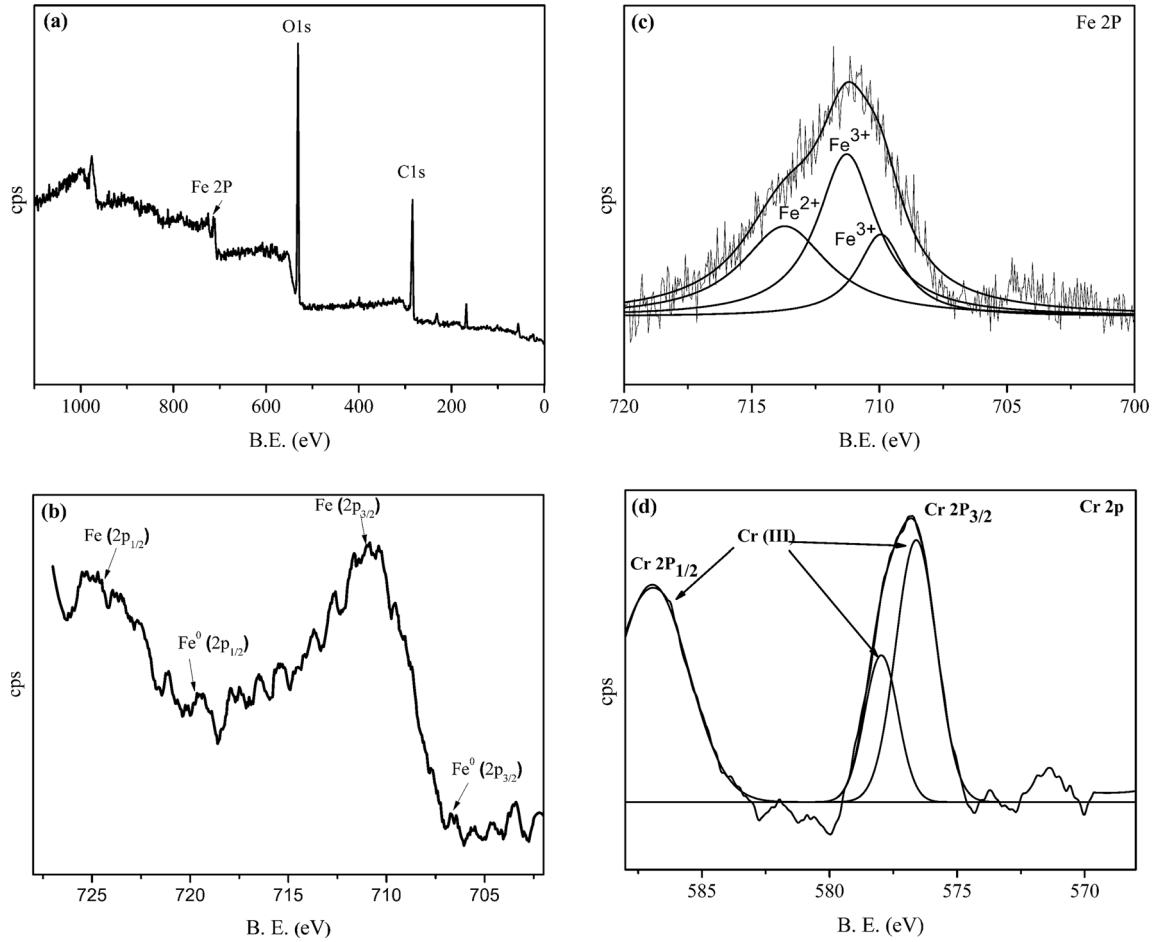

Fig. 7 XPS spectrum of biomaterial CL-FeNPs and biomaterial treated with chromium solution. **a** Wide scan survey of biomaterial CL-FeNPs, **b** XPS survey on Fe 2P core shell before treatment with chromium solution, **c** XPS survey on Fe 2P core shell after treatment with chromium solution and **d** XPS survey of Cr 2P core shell after treatment with chromium solution

size of iron particles was found to be 124 nm. The large size of iron particles was due to the agglomeration of iron which is highly reactive in nature. Increase in extract volume increases the iron particle concentration for fixed initial chromium concentration 2500 mg L^{-1}. Complete reduction was attained for 6 mL of Fe dispersed liquid extract for 20 mL of chromium stock solution whereas 1.5 g of biomaterial CL-FeNPs was sufficient for the complete reduction of Cr(VI) for same volume of stock solution. Though the quantity of iron is high in the liquid extract, the size of iron is high with higher oxidation state indicating lower capacity of chromium reduction.

Comparative study between freshly prepared and regenerated biomaterial

For a comparative study, equal volume of stock solution i.e. 100 mL of 1000 mg L^{-1} concentration was taken in two beakers and 2.5 g of freshly prepared biomaterial CL-FeNPs, and regenerated biomaterial was added to respective beakers. For regeneration of biomaterial, used biomaterial was retreated with liquid extract at optimum pH of 4. Regeneration process includes reduction of precipitated iron(III) oxides in biomass into iron(II) oxide and metallic iron. H^+ ions and reducing agents from biomass help in reduction of iron(III) oxide which makes CL-FeNPs reusable. Experiments were performed for different residence times of 10, 20, and 30 min. From Fig. 5, it was observed that 90% reduction was attained for freshly prepared sample and 80% reduction was attained for regenerated sample. The experimental results convey that biomaterial CL-FeNPs can be regenerated which would compete with percentage reduction of Cr(VI) $80 \pm 3\%$ with fresh biomaterial.

Kinetic analysis

From the experimental data obtained for reduction of chromium(VI) solution with time, kinetic analysis was performed. Due to the instantaneous reduction of the adsorbed (Cr^{6+}), the rate expression of the shifting order was proposed

$$-r_A = \frac{k_1 C_A}{1 + k_2 C_A} \tag{3}$$

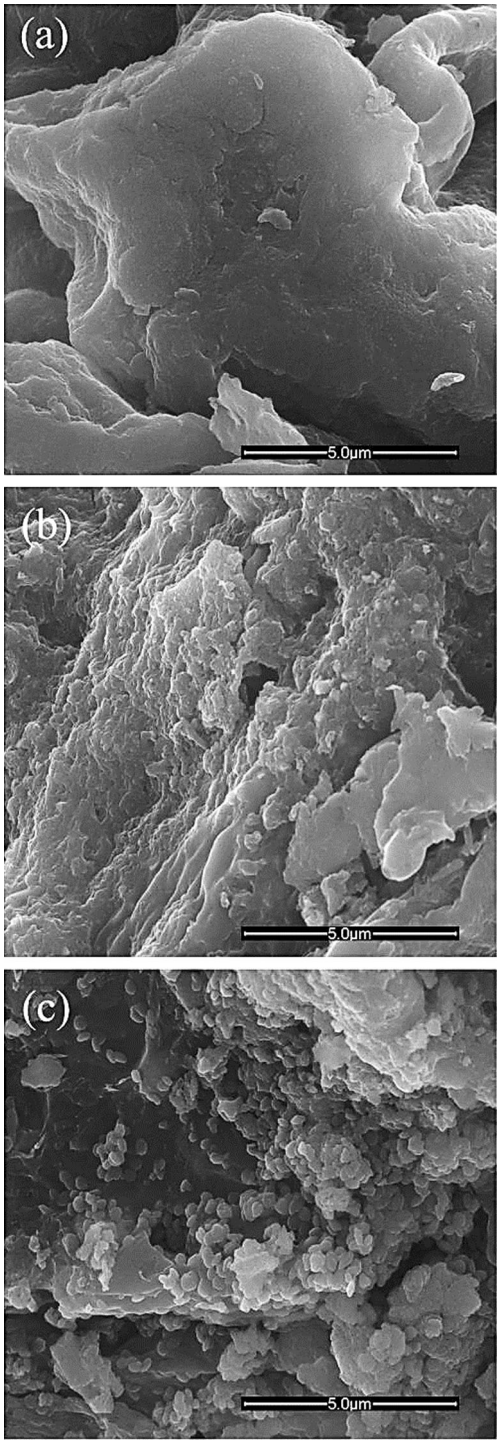

Fig. 8 FESEM imaging **a** fresh *Citrus limetta* peels, **b** biomaterial treated with metal salt, **c** treated biomaterial after contact with chromium solution

At very high concentrations, the reaction follows zero order while at lower concentrations it follows first order with respect to time. Upon the regression with the generated experimental data, the following kinetic parameters k_1 = 120.93 mg L^{-1} min^{-1}; $k_2 = 0.0729$ min^{-1} with $R^2 = 0.9915$ was obtained.

Characterisation

To find out the crystallinity of CL-FeNPs, X-ray diffraction was performed and the results were analysed using PAN analytical X'pert High score software. From Fig. 6, it was observed that the biological synthesis lead to the production of amorphous iron nanoparticles resulting no peaks. Similar results were reported using plant extracts such as green tea (Machado et al. 2013), eucalyptus bark and sorghum bran (Njagi et al. 2011). The peak between 20° to 30° of 2θ values was due to the presence of cellulosic content and other organics which acts as capping agent for synthesis of nanoparticles (Zhou et al. 2014). XRD of biomaterial after contact with chromium was also analysed. From XRD analysis, the presence of Cr(III) was confirmed in the form of Cr_2O_3 (JCPDS file no. 38-1479) while other peaks were noted to be the oxides of iron as Fe_2O_3 (JCPDS file no. 85-0987) and Fe_3O_4 (JCPDS file no. 85-1436). This confirms the reduction of Cr(VI) to Cr(III) and oxidation of iron from Fe^0 to higher oxidation state at the contact.

To determine the oxidation state of iron in CL-FeNPs, XPS analysis was performed at Fe 2p core levels. Figure 7a shows wide scan survey of biomaterial which confirms the presence of O, C and Fe while Fig. 7b shows the Fe $2p_{3/2-1/2}$ core levels for iron nanoparticles. The binding energies at 706.9 eV and 719.8 are characteristic peaks for metallic iron whereas wide peaks corresponding to 710.8 eV and 724.5 eV were iron oxides (Zhou et al. 2014). This confirms the presence of zero-valent state of iron nanoparticles through XPS analysis. The main forms of Fe in the developed material were Fe^0 and Fe^{2+}. Figure 7c and d shows the XPS analysis of treated biomaterial with chromium solution. Upon the treatment with chromium solution, iron nanoparticles which were Fe^0 and Fe^{2+} would be converted to Fe^{3+}. Figure 7c shows the convoluted peaks of Fe of different oxidation states Fe^{3+} and Fe^{2+}. The peaks of XPS of Fig. 7c confirm the transformation of Fe^0 to Fe_2O_3 and Fe_3O_4. Broad peak of Fe_3O_4 in comparison with peak of Fe_2O_3 suggests that Fe_3O_4 was the main form of species in the final treated material. From Fig. 7d, binding energies at 586.1, 576.3 and 578.3 eV confirm the presence of Cr(III) in the form of chromium(III) oxide and chromium hydroxide (Mary Mangaiyarkarasi et al. 2011; Song et al. 2015). This confirms that Cr(VI) gets reduced to Cr(III) with the synthesised nanometal induced biomaterial with the following reactions (Eqs. (4) and (5)).

$$Fe^0 + Cr_2O_7^- + 4H_2O \rightarrow Fe^{2+} + 2Cr(OH)_3 + 8OH^{-1} \quad (4)$$

$$6Fe^{2+} + Cr_2O_7^- + 14H^+ \rightarrow 6Fe^{3+} + 2Cr^{3+} + 7H_2O \quad (5)$$

The analysis of surface morphology, elemental distribution and imaging was done through FESEM. SEM micrographs

and EDS spectra indicates the elemental distribution as shown in Fig. 8 and Fig. 9 respectively. SEM imaging depicts the change in morphology of washed sample (Fig. 8a) and the treated sample (Fig. 8b). Washed sample appeared to be fibrous and smooth while the treated sample appeared to be rough resulting an increase in the surface area (SA_{BET} = 6.2 m^2/g) due to the reaction with metal salt. From EDS, it was reported that iron content was 29.95 wt% (9.92 atomic %) as shown in Fig. 9a.

Biomaterial CL-FeNPs after reaction with Cr(VI) solution was also analysed through SEM. SEM imaging reveals that there are formation of aggregates which are spherical in shape as shown in Fig. 8c. EDS spectrum of the aggregates shows the presence of iron content about 28 wt% (9.54 atomic %) and chromium of nearly 0.03 wt% (0.01 atomic %) as shown in Fig. 9b. The traces of chromium on the surface of biomaterial indicate the low binding of Cr(III) after oxidation of iron nanoparticles. Further, these lower chromium concentrations infer that reduced Cr(III) got desorbed into solution after reduction.

HRTEM was used to determine the size and shape of the iron nanoparticles. Figure 10 shows that the nanoparticles are spherical in shape and were polydisperse. Distribution of iron nanoparticles has been widespread ranging from 4 to 70 nm. Iron nanoparticles are highly reactive which tends to agglomerate and gets easily oxidised in an open environment (Geng et al. 2009). The synthesised nanoparticles supported on peels hamper the oxidation when kept in an open atmosphere confirming the stability of the particles.

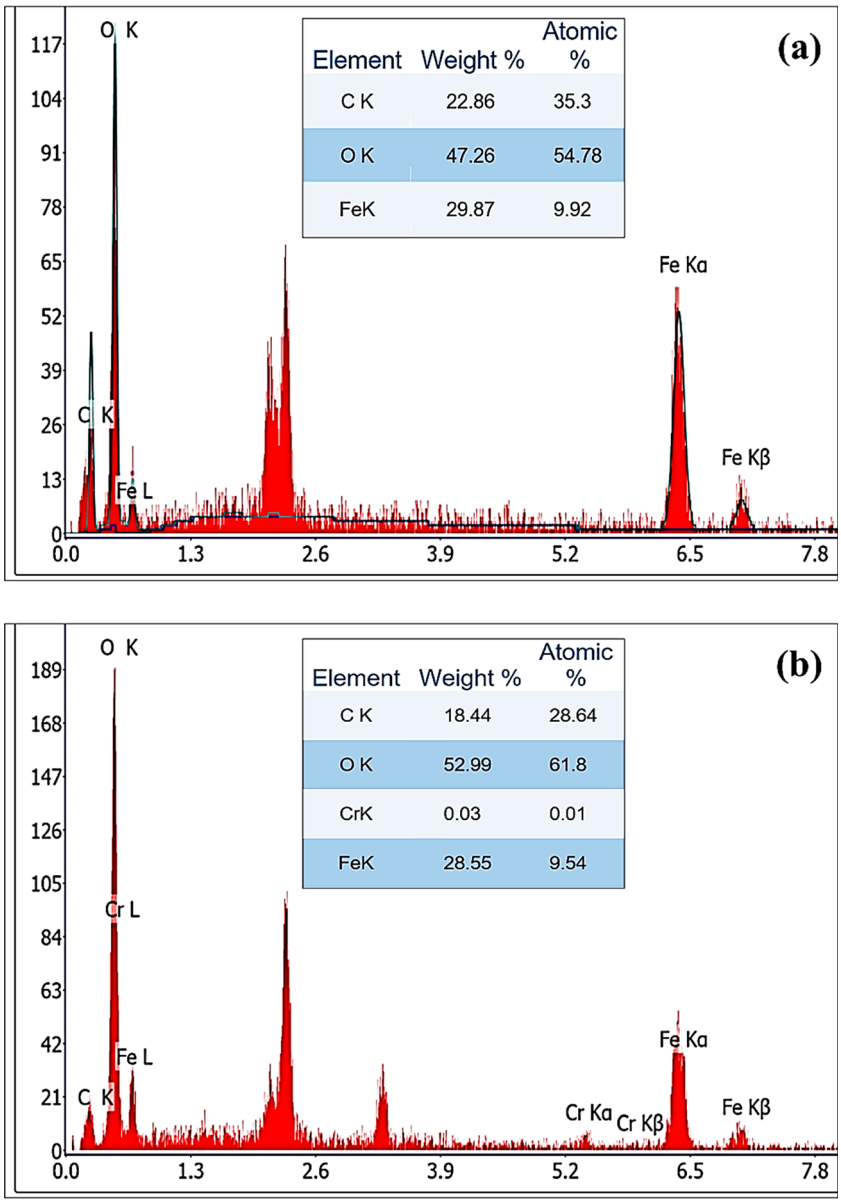

Fig. 9 EDS spectra indicating metal composition **a** biomaterial treated with metal salt, **b** treated biomaterial after contact with chromium solution

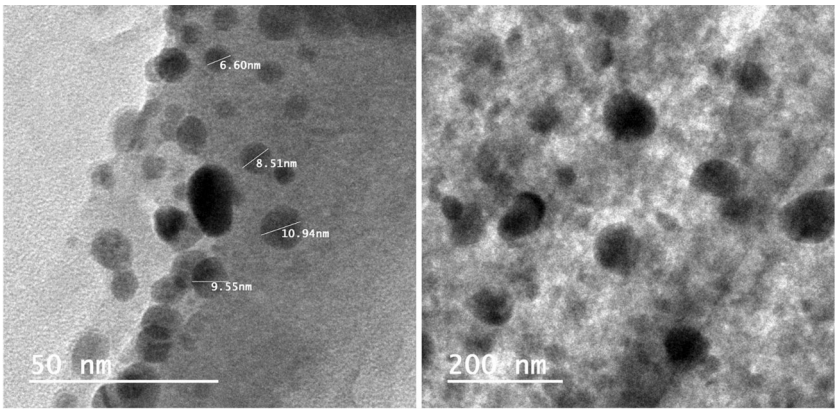

Fig. 10 HRTEM images of biomaterial CL-FeNPs showing iron nanoparticles entrapped in biomass

Conclusions

In this study, iron nanoparticles were successfully embedded in the *Citrus limetta* using green technique. Batch experiments revealed that the reduction of Cr(VI) to Cr(III) increased with the increase of CL-FeNPs and decreased when initial Cr(VI) concentration increased. Complete Cr(VI) reduction was observed for 2500 mg L^{-1} and a maximum reduction capacity of 33.3 mg/g was attained. Characterisation was done for both freshly prepared and treated biomaterial after contact with chromium solution. The amorphous nature with high dispersion and nanosize of iron in *Citrus limetta* peels makes it as a novel material for the reduction process. Zero-valent state of iron in the synthesised CL-FeNPs paves the path for high reduction of toxic hexavalent chromium. This novel biomaterial shows a great potential for the reduction of toxic metals in industrial wastewaters.

References

Bhattacharyya KG, Gupta SS (2008) Adsorption of a few heavy metals on natural and modified kaolinite and montmorillonite: a review. Adv Colloid Interf Sci 140:114–131. https://doi.org/10.1016/j.cis.2007.12.008

Chen L, Ji T, Mu L, Shi Y, Brisbin L, Guo Z, Khan MA, Young DP, Zhu J (2016) Facile synthesis of mesoporous carbon nanocomposites from natural biomass for efficient dye adsorption and selective heavy metal removal. RSC Adv 6:2259–2269. https://doi.org/10.1039/c5ra19616g

Costa M, Klein C (2006) Toxicity and carcinogenicity of chromium compounds in humans. CRC Crit Rev Toxicol 36:155–163. https://doi.org/10.1080/10408440500534032

Dharnaik AS, Ghosh PK (2014) Hexavalent chromium [Cr(VI)] removal by the electrochemical ion-exchange process. Environ Technol (United Kingdom) 35:2272–2279. https://doi.org/10.1080/09593330.2014.902108

Ebrahiminezhad A, Zare-Hoseinabadi A, Berenjian A, Ghasemi Y (2017) Green synthesis and characterization of zero-valent iron nanoparticles using stinging nettle (Urtica dioica) leaf extract. Green Process Synth 6. https://doi.org/10.1515/gps-2016-0133

Fahmy HM, Mohamed FM, Marzouq MH, Mustafa ABED, Alsoudi AM, Ali OA, Mohamed MA, Mahmoud FA (2018) Review of green methods of iron nanoparticles synthesis and applications. Bionanoscience 8:491–503. https://doi.org/10.1007/s12668-018-0516-5

Gaikwad MS, Balomajumder C (2018) Removal of Cr(VI) and fluoride by membrane capacitive deionization with nanoporous and microporous Limonia acidissima (wood apple) shell activated carbon electrode. Sep Purif Technol 195:305–313. https://doi.org/10.1016/j.seppur.2017.12.006

Gan PP, Li SFY (2012) Potential of plant as a biological factory to synthesize gold and silver nanoparticles and their applications. Rev Environ Sci Biotechnol 11:169–206. https://doi.org/10.1007/s11157-012-9278-7

Garg UK, Kaur MP, Sud D, Garg VK (2009) Removal of hexavalent chromium from aqueous solution by adsorption on treated sugarcane bagasse using response surface methodological approach. Desalination 249:475–479. https://doi.org/10.1016/j.desal.2008.10.025

Geng B, Jin Z, Li T, Qi X (2009) Kinetics of hexavalent chromium removal from water by chitosan-Fe0 nanoparticles. Chemosphere 75:825–830. https://doi.org/10.1016/j.chemosphere.2009.01.009

Hoag GE, Collins JB, Holcomb JL, Hoag JR, Nadagouda MN, Varma RS (2009) Degradation of bromothymol blue by "greener" nano-scale zero-valent iron synthesized using tea polyphenols. J Mater Chem 19:8671–8677. https://doi.org/10.1039/b909148c

Johnson P, Loganathan C, Krishnan V, Sakayanathan P, Raji V, Vijayan S, Sathishkumar P, Murugesan K, Palvannan T (2017) Plant extract as environmental-friendly green catalyst for the reduction of hexavalent chromium in tannery effluent. Environ Technol (United Kingdom) 3330:1–8. https://doi.org/10.1080/09593330.2017.1329355

Karthikeyan T, Rajgopal S, Miranda LR (2005) Chromium(VI) adsorption from aqueous solution by Hevea Brasilinesis sawdust activated carbon. J Hazard Mater 124:192–199. https://doi.org/10.1016/j.jhazmat.2005.05.003

Kim T, Kim T, Choe W, Kim MK, Jung YJ, Zoh KD (2018) Removal of heavy metals in electroplating wastewater by powdered activated carbon (PAC) and sodium diethyldithiocarbamate-modified PAC. Environ Eng Res 23:301–308

Kumari V, Sasidharan M, Bhaumik A (2015) Mesoporous $BaTiO_3$@SBA-15 derived via solid state reaction and its excellent adsorption efficiency for the removal of hexavalent chromium from water. Dalt Trans 44:1924–1932. https://doi.org/10.1039/c4dt03180f

Li XQ, Elliott DW, Zhang WX (2006) Zero-valent iron nanoparticles for abatement of environmental pollutants: materials and engineering

aspects. Crit Rev Solid State Mater Sci 31:111–122. https://doi.org/10.1080/10408430601057611

Li Z, Kirk Jones H, Zhang P, Bowman RS (2007) Chromate transport through columns packed with surfactant-modified zeolite/zero valent iron pellets. Chemosphere 68:1861–1866. https://doi.org/10.1016/j.chemosphere.2007.03.011

López-Téllez G, Barrera-Díaz CE, Balderas-Hernández P, Morales GR, Bilyeu B (2011) Removal of hexavalent chromium in aquatic solutions by iron nanoparticles embedded in orange peel pith. Chem Eng J 173:480–485. https://doi.org/10.1016/j.cej.2011.08.018

Machado S, Pinto SL, Grosso JP, Nouws HPA, Albergaria JT, Delerue-Matos C (2013) Green production of zero-valent iron nanoparticles using tree leaf extracts. Sci Total Environ 445–446:1–8. https://doi.org/10.1016/j.scitotenv.2012.12.033

Madhavi V, Prasad TNVKV, Reddy AVB, Reddy R, Madhavi G (2013) Application of phytogenic zerovalent iron nanoparticles in the adsorption of hexavalent chromium. Spectrochim Acta A Mol Biomol Spectrosc 116:17–25. https://doi.org/10.1016/j.saa.2013.06.045

Mary Mangaiyarkarasi MS, Vincent S, Janarthanan S, Subba rao T, Tata BVR (2011) Bioreduction of Cr(VI) by alkaliphilic Bacillus subtilis and interaction of the membrane groups. Saudi J Biol Sci 18:157–167. https://doi.org/10.1016/j.sjbs.2010.12.003

Miretzky P, Cirelli AF (2010) Cr(VI) and Cr(III) removal from aqueous solution by raw and modified lignocellulosic materials: a review. J Hazard Mater 180:1–19. https://doi.org/10.1016/j.jhazmat.2010.04.060

Narayanan KB, Sakthivel N (2010) Biological synthesis of metal nanoparticles by microbes. Adv Colloid Interf Sci 156:1–13. https://doi.org/10.1016/j.cis.2010.02.001

Nayak A, Bhushan B, Gupta V, Sharma P (2017) Journal of colloid and interface science chemically activated carbon from lignocellulosic wastes for heavy metal wastewater remediation: effect of activation conditions. J Colloid Interface Sci 493:228–240. https://doi.org/10.1016/j.jcis.2017.01.031

Njagi EC, Huang H, Stafford L, Genuuino H, Galindo HM, Collins JB, Hoag GE, Suib SL (2011) Biosynthesis of iron and silver nanoparticles at room temperature using aqueous sorghum bran extracts. Langmuir 27:264–271. https://doi.org/10.1021/la103190n

Ray S, Kanti Ray M (2009) Bioremediation of heavy metal toxicity-with special reference to chromium. Al Ameen J Med Sei 2:57–63

Richardson Y, Blin J, Volle G, Motuzas J, Julbe A (2010) In situ generation of Ni metal nanoparticles as catalyst for H2-rich syngas production from biomass gasification. Appl Catal A Gen 382:220–230. https://doi.org/10.1016/j.apcata.2010.04.047

Sathishkumar M, Sneha K, Yun YS (2010) Immobilization of silver nanoparticles synthesized using Curcuma longa tuber powder and extract on cotton cloth for bactericidal activity. Bioresour Technol 101:7958–7965. https://doi.org/10.1016/j.biortech.2010.05.051

Song Z, Li W, Liu W, Yang Y, Wang N, Wang H, Gao H (2015) Novel magnetic lignin composite sorbent for chromium(VI) adsorption. RSC Adv 5:13028–13035. https://doi.org/10.1039/c4ra15546g

Thakur S, Karak N (2014) One-step approach to prepare magnetic iron oxide/reduced graphene oxide nanohybrid for efficient organic and inorganic pollutants removal. Mater Chem Phys 144:425–432. https://doi.org/10.1016/j.matchemphys.2014.01.015

Vivek Narayanan N, Ganesan M (2009) Use of adsorption using granular activated carbon (GAC) for the enhancement of removal of chromium from synthetic wastewater by electrocoagulation. J Hazard Mater 161:575–580. https://doi.org/10.1016/j.jhazmat.2008.03.113

Yin W, Li Y, Wu J, Chen G, Jiang G, Li P, Gu J, Liang H, Liu C (2017) Enhanced Cr(VI) removal from groundwater by Fe^0-H2O system with bio-amended iron corrosion. J Hazard Mater 332:42–50. https://doi.org/10.1016/j.jhazmat.2017.02.045

Yuan P, Liu D, Fan M, Yang D, Zhu R, Ge F, Zhu J, He H (2010) Removal of hexavalent chromium [Cr(VI)] from aqueous solutions by the diatomite-supported/unsupported magnetite nanoparticles. J Hazard Mater 173:614–621. https://doi.org/10.1016/j.jhazmat.2009.08.129

Zhou S, Li Y, Chen J, Liu Z, Wang Z, Na P (2014) Enhanced Cr(VI) removal from aqueous solutions using Ni/Fe bimetallic nanoparticles: characterization, kinetics and mechanism. RSC Adv 4:50699–50707. https://doi.org/10.1039/c4ra08754b

Zhou L, Li R, Zhang G, Wang D, Cai D, Wu Z (2018) 2018 Zero-valent iron nanoparticles supported by functionalized waste rock woolfor efficient removal of hexavalent chromium. Chem Eng J 339:85–96. https://doi.org/10.1016/j.cej.2018.01.132